Encapsulation of Human IgG Antibody in PLGA Microparticles Fabricated by Coaxial Electrospray

Karla Nataly Robles * , John Paul Libanati , Richard Mu , Todd Giorgio

Posted Date: 21 May 2024

doi: 10.20944/preprints202405.1354.v1

Keywords: antibody encapsulation; sustained-release; PLGA; immunotherapy; local administration; microparticles; coaxial electrospray

Article

Encapsulation of Human IgG Antibody in PLGA Microparticles Fabricated by Coaxial Electrospray

Karla N. Robles [1,*], John Paul Libanati [2], Richard Mu [1] and Todd Giorgio [2]

[1] TIGER Institute, Tennessee State University
[2] Department of Biomedical Engineering, Vanderbilt University
* Correspondence: karlanatalyrobles@gmail.com

Abstract: Advances in the treatment of cancer with immunotherapy necessitate a locally administered sustained-delivery system to improve treatment efficacy and reduce toxicity. Towards this end, the encapsulation and release characteristics of human antibody immunoglobulin-G (IgG-FITC) were investigated with the coaxial electrospray technique. The antibody solution was exchanged for a solution at the antibody's isoelectric pH. The shell solution consisted of PLGA in ethyl acetate. The impact of shell flow rates was investigated in the fabrication of IgG-FITC-loaded PLGA microparticles and the release-profile of IgG-FITC from the PLGA microparticles was characterized. Encapsulation efficiency ranged from 0.04-1.52%. Fluorescence images suggest core localization in the formulation with a lower shell flow rate and shell localization in the formulation with the higher shell flow rate. SEM image analysis revealed that lower shell flow rate resulted in the smaller average particle size with minimal difference in zeta potential between formulations. The lower shell flow rate exhibited a release profile with a $t_{1/2}$ of 36 hours whereas the higher shell flow rate had a $t_{1/2}$ < 3 hours. Antibody-fluorescence signals were measured for 28 days and indicated a biphasic release profile with a burst-release followed by a sustained-release in both formulations.

Keywords: antibody encapsulation; sustained-release; PLGA; immunotherapy; local administration; microparticles; coaxial electrospray

1. Introduction

Cancer immunotherapy is a powerful treatment that activates the immune system of the patient to combat the tumor. Systemic administration of immunotherapy can result in adverse off-target effects, so sustained delivery of immunotherapy following local administration is a promising alternative [1]. Immune checkpoint blockade is a form of immunotherapy that employs monoclonal antibodies such as anti-programmed cell death protein 1 and anti-programmed cell death protein-ligand 1 (anti-PD-1/anti-PD-L1). Current studies have shown promise in controlled-release antibodies for tumor immune checkpoint blockade [2,3]. However, antibody encapsulation technology is new and antibody payload release dynamics have not been fully explored. Recently developed antibody delivery systems and delivery technologies for the immunotherapy of cancer are reviewed here [4,5].

Therapeutic reservoir and drug-polymer matrix systems can extend the delivery of therapies and reduce risk of dose toxicity [6,7]. Typically, these drug-delivery systems consist of a drug payload encapsulated within a polymeric carrier, and the delivery mechanism(s) by which the drug payload is released. Release mechanisms are categorized via payload diffusion, payload-carrier disintegration, polymer swelling, stimuli responsiveness (e.g., pH-activated release), and polymer erosion and degradation [7].

Poly(lactic-*co*-glycolic acid), or PLGA, is an FDA approved biodegradable copolymer with extensive applications as a drug-delivery carrier [8–10]. PLGA is composed of lactic acid and glycolic acid monomers. It is characterized by its molecular weight, monomer ratios, and end groups. PLGA

 doi:10.20944/preprints202405.1354.v1

degrades by hydrolysis of the ester bonds of its monomers. It is an attractive polymer for drug-delivery because its molecular weight and monomer ratio can be tuned to modify payload release dynamics. The hydrolysis products are nontoxic and excreted in mammalian systems.

One challenge of many PLGA-based carriers is the tendency to initially release a disproportionately large fraction of the drug cargo [11,12]. This phenomenon is called 'burst release' and is generally disfavored when a uniform, sustained release profile is desired. Additionally, challenges in the encapsulation of antibodies in microparticles are due, in part, to the hydrophilic nature of the payload and hydrophobicity of the encapsulating polymer(s). Strategies for improving the encapsulation of small hydrophilic molecules in PLGA microparticles have been outlined for emulsion fabrication, spray-drying, and inkjet printing techniques [13].

PLGA-alginate microspheres for hydrophilic protein delivery were reported by Zhai *et al,* (2015). A double emulsion and solvent evaporation technique was employed to fabricate PLGA and PLGA-alginate microparticles with hydrophilic protein, bovine serum albumin (BSA). The same technique was used to load PLGA and PLGA-alginate microparticles with rabbit anti-laminin antibody, another protein. The incorporation of alginate in the PLGA particles was reported to provide a more sustained release profile compared to PLGA particles, though PLGA-alginate particles had a reduced biocompatibility [14]. In a separate study, protein-loaded PLGA-alginate particles were fabricated with a water-in-oil emulsification and external gelation. The process parameters, including alginate concentration, cross-linking time, and drying time of BSA-loaded PLGA-alginate particles, were optimized to provide a 13% reduction of the BSA burst-release [15]. However, conventional emulsification techniques risk exposure of the biomolecule payload to organic solvents during fabrication with the potential for loss of bioactivity.

The electrohydrodynamic atomization technique (EHDA), or electrospray, has been used to fabricate single-layer polymeric microstructures from particles and fibers to films at a range of scales (nano to micro) for drug-delivery [12]. A polymeric solution is pumped through a steel needle and a voltage is applied. In the presence of a high voltage, the solution droplet at the tip of the needle deforms into a Taylor cone from which a microjet emerges. As the electric charge builds up on the surface of the polymeric solution and overcomes the Rayleigh limit, the solution breaks off into microdroplets. The solvent evaporates from the microdroplets descend, and microparticles are collected on a ground collector. --

Coaxial electrospray is an extension of the electrospray technique in which a core payload solution is dispensed to an inner capillary and the shell solution is dispensed to an outer capillary. Complex hydrophilic-in-hydrophobic and multi-layer microstructures have been manufactured using this technique [16]. Microparticles have been produced using coaxial electrospray with poly(L-lactic acid) (PLA) with hydrophilic drug core and PLGA with hydrophobic drug shell in dichloromethane (DCM) and ethyl acetate solvents, respectively [16]. The inverse core-shell configuration was also fabricated. A follow-up study showed the encapsulation of two drugs with different degrees of hydrophilicity, paclitaxel and suramin, in PLA and PLGA microspheres to treat mouse U87 glioma [17]. Hydrophilic protein encapsulation in microparticles and fibers with electrospray and electrospinning is reviewed here [18].

The optimization of electrospray parameters can facilitate the fabrication of monodisperse and microstructures [19]. For example, the polymer concentration in the shell solution affects the size and thickness of the particles fabricated. Similarly, the shell flow rate impacts the particle size and shell thickness. The effect of an increased shell flow rate on release profile of curcumin has been shown to reduce burst release and delay release by increasing microparticle shell thickness [20].

Since particle fabrication with electrospray requires the presence of an electric field, a net charge of the drug payload solution can affect its localization within the particle. This is important to consider towards encapsulating proteins and antibodies with this technology. In an electrospinning study, BSA was localized in the core of polyvinyl alcohol (PVA) fibers when dissolved at its isoelectric point [21]. In another study, antibody-encapsulation of bevacizumab in poly-caprolactone (PCL) fibers was achieved using coaxial electrospinning for sustained-release treatment of age-related macular degeneration. The authors showed a first-order antibody release profile with $t_{1/2}$ of 11 days

 doi:10.20944/preprints202405.1354.v1

from PCL nanofibers fabricated at the commercial pH and transmission electron microscopy (TEM) images suggested antibody localization in the shell. Comparatively, a zero-order release profile with a $t_{1/2}$ of 52 days was achieved at the antibody's isoelectric point and TEM images suggest antibody localization in the core [22].

To date, coaxial electrospray has not been used to fabricate antibody-loaded PLGA microparticles. Thus, there is a gap in the knowledge of electrospray parameters which can achieve antibody encapsulation in PLGA microparticles and characterization of the resultant antibody release profiles. In this manuscript, we focus on the effect of shell flow rate on antibody encapsulation and antibody release-profile which has not been reported previously in the literature. Fluorescent human immunoglobulin-G (IgG-FITC) antibody was used because it is an isotype of various antibodies used in immune checkpoint blockade. We present the development of human antibody-loaded PLGA microparticles using coaxial electrospray at the antibody's isoelectric point.

2. Materials and Methods

2.1. Materials

Resomer® RG 504 H, Poly(D,L-lactide-co-glycolide) (PLGA) (L:G 50:50, M_w: 38-54 kDa, acid-terminated), immunoglobulin-G (IgG)-FITC from human serum (20 mg/mL), ethyl acetate (ACS reagent, 99.5%), Trizma® Pre-set crystals pH 8.5, phosphate buffered saline (PBS) pH 7.4, Amicon® Ultra Centrifugal Filter (30 kDa MWCO, 2 mL), and poly(vinyl alcohol) (PVA) M_w: 9,000-10,000), were purchased from Millipore Sigma.

2.2. Isoelectric Point of Human Immunoglobulin-G1

The amino acid sequence of the IgG1 antibody was retrieved from the DrugBank database, and the isoelectric point, *pI*, was calculated using the SIB Swiss Institute of Bioinformatics pI M_w tool. The detailed output can be found in Supplementary Figure S1.

2.2. Preparation of Solutions for Coaxial Electrospray

The concentrations of the solutions are summarized in Table 1. 50 mg/mL of PLGA was dissolved in ethyl acetate for the shell solution. To prepare the core solution (Figure 1a), 1 mL of IgG-FITC from human serum (20 mg/mL) was placed into an Amicon® Ultra Centrifugal Filter (30 kDa MWCO) and centrifuged for 30 minutes to extract the PBS solvent at pH 7.4. Separately, Trizma® pre-set crystals were dissolved in DI water to achieve the *pI* buffer with pH 8.5. The antibody recovered from centrifugation was diluted to a concentration of 10 mg/mL using the *pI* buffer.

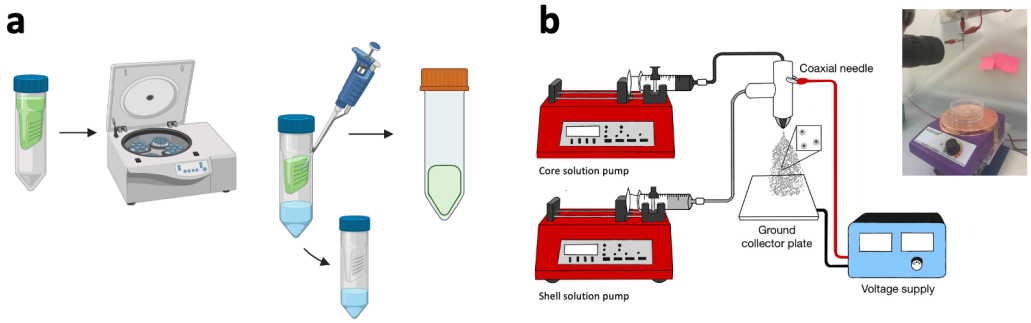

Figure 1. (**a**) Centrifugal ultrafiltration of IgG-FITC for solvent-exchange. The IgG-FITC solution is placed in a centrifugal ultrafiltration column. The solvent is extracted through centrifugation, and the IgG-FITC is retrieved and dissolved in the *pI* buffer. (**b**) Coaxial electrospray system for microparticle fabrication. The IgG-FITC *pI* solution is pumped as the core solution, and the PLGA solution is pumped as the shell solution.

 doi:10.20944/preprints202405.1354.v1

Table 1. Experimental conditions used in coaxial electrospray of IgG-FITC and PLGA solutions for the fabrication of antibody-loaded microparticles.

Core solution	Shell solution	Formulation	Core flow rate (mL/hr)	Shell flow rate (mL/hr)	Voltage	Distance to collector
10 mg/mL IgG-FITC at pH 8.5 aqueous	50 mg/mL PLGA in ethyl acetate	1	0.05	0.5	8.5 kV	15 cm
		2	0.05	2.0		

2.3. Fabrication of Antibody-Loaded PLGA Microparticles with Coaxial Electrospray

The parameters used to fabricate the antibody-loaded microparticles are summarized in Table 1 and the coaxial electrospray system is shown in Figure 1b. Individual syringe pumps were used to dispense the inner and outer solutions at 0.05 mL/hr and 0.5-2 mL/hr, respectively. The solutions were pumped into a 23/17 G coaxial steel needle. A voltage difference of 8.5 kV was applied between the needle and the collector. The microparticles were sprayed onto a ground collector located 15 cm below the needle tip. The microparticles were collected in a stirred deionized (DI) water bath containing 1% PVA. The antibody-loaded microparticles recovered from the DI water-PVA bath were kept atn 4°C for 12 hours for shell hardening, then washed three times by centrifugation in DI water containing 1% PVA. The particles were lyophilized for 24 h using BUCHI Lyovapor™ L-200 Freeze Dryer. Dried particles were stored at –4 °C prior to characterization and release kinetics analysis.

2.4. Characterization of Antibody-Loaded PLGA Microparticles

5 µL of microparticles in DI water were pipetted onto a glass slide and imaged using a Keyence All-in-one microscope. Brightfield and fluorescence images were collected at 40x to investigate colocalization of the microparticles with the fluorescent antibody. Microparticle morphology was imaged with a Zeiss Merlin scanning electron microscope (SEM). Size distribution of the microparticles captured by SEM was determined using ImageJ. Specifically, the circumference (C) and diameters of the (D_M) major and minor axes (D_m) of 50 particles from each preparation were manually identified. Particle zeta potential was analyzed using a Malvern Panalytical Zetasizer Advance Range.

2.5. Characterization of Antibody Release Profile from Antibody-Loaded PLGA Microparticles

In vitro release kinetics were measured by incubating microparticles at 37°C in 1 mL of 1% PBS/BSA buffer solution with a pH of 7.4 (Figure 2). At each time point, the particle suspension was centrifuged at 10x g for 10 minutes at 10°C. Supernatant was extracted and its fluorescence was analyzed relative to an IgG-FITC standard curve using a Tecan Infinite M1000Pro plate reader to calculate the degree of antibody release by the microparticles. After extraction, the supernatant was replaced with 1 mL of 1% PBS/BSA buffer, and the tube was vortexed to resuspend the particles before it was placed back in the incubator.

 doi:10.20944/preprints202405.1354.v1

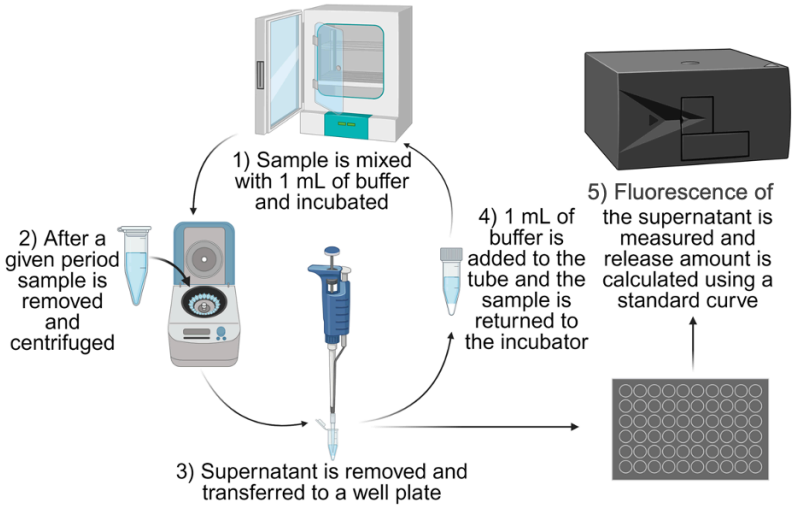

Figure 2. Protocol for quantification of antibody release from microparticles through fluorescence measurements. The antibody-loaded microparticles were incubated in PBS pH 7.4, then centrifuged and fluorescence measurements of the supernatant were collected at each time point.

3. Results

3.1. Morphology and Fluorescence of Antibody-Loaded PLGA Microparticles

Figure 3 is a set of SEM images of microparticles fabricated with the coaxial electrospray method showing non-spherical, round, and sunken particle structure for Formulation 1 (Figure 3a), and discoidal and round particle structure for Formulation 2 (Figure 3b). Optical microscope images and fluoresecence images suggest colocalization of particles and antibody fluoresence signal. In Formulation 1, the fluoresence image suggests antibody core localization whereas in Formulation 2, the fluoresence image suggests antibody shell localization. Table 2 summarizes the averages of particle size and zeta potential for each formulation. Formulation 1 demonstrates lower average circumference as well as major and minor axis size than Fomulation 2 (Table 2). Both particles exhibit a similar negative zeta potential (Table 2).

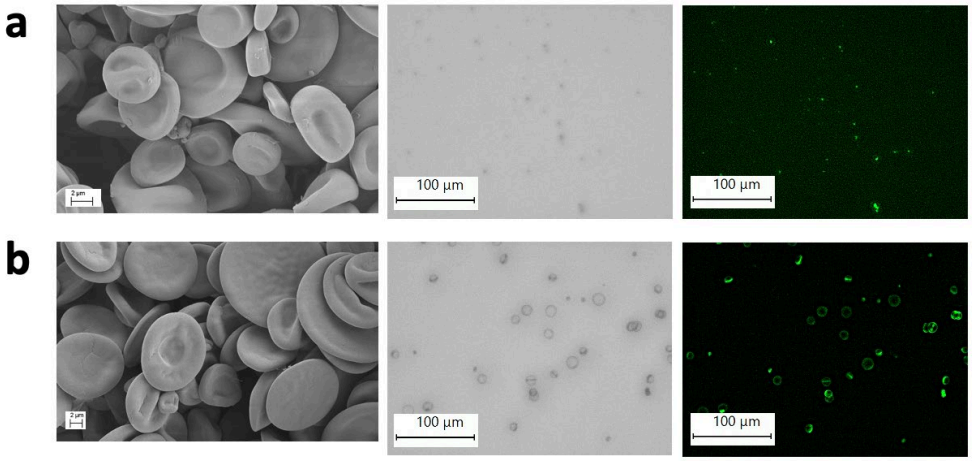

Figure 3. SEM, optical (40x), and fluorescence (40x) images of microparticles with shell flow rates of (**a**) 0.5 mL/hr and (**b**) 2.0 mL/hr.

 doi:10.20944/preprints202405.1354.v1

Table 2. Measurements of circumference (C), major axis diameter (D_M), minor axis diameter (Dm), and zeta potential taken from SEM images of Formulation 1 and Formulation 2 particles.

Formulation	C (μm)	Standard Deviation (μm)	D_M (μm)	Standard Deviation (μm)	D_m (μm)	Standard Deviation (μm)	Zeta Potential (mV)
1	28.30	32.54	8.34	5.72	6.64	4.55	-29.15
2	34.54	39.94	10.6	4.80	9.36	4.97	-35.85

3.2. Encapsulation Efficiency of Antibody-Loaded PLGA Microparticles

Fluoresence measurements of the particles analyzed according to Figure 2 were used to calculate encapsulation efficiency (EE). The EE was calculated as the percent of total mass of IgG-FITC released from the PLGA particles at the end of the experiments divided by the amount of IgG-FITC used in the electrospray fabrication of the particles.

$$EE\ (\%) = \frac{Total\ antibody\ released\ from\ PLGA\ particles}{Total\ antibody\ used\ in\ electrospray\ fabrication} \times 100\ \%$$

Formulation 1 and Formulation 2 had encapsulation efficiencies of $0.04 \pm 0.01\%$ and $1.52 \pm 0.23\%$, respectively.

3.3. Fluorescence Release Profile of Antibody-Loaded PLGA Microparticles

Figure 4 shows the percent release of IgG-FITC ng per mg of particles. The release profile of Formulation 1 shows a $t_{1/2}$ of 36 hours compared to Formulation 2 with a $t_{1/2} < 3$ hours. Antibody-fluoresence signals measured for 28 days indicated a biphasic release profile with a burst-release followed by a sustained-release for both formulations.

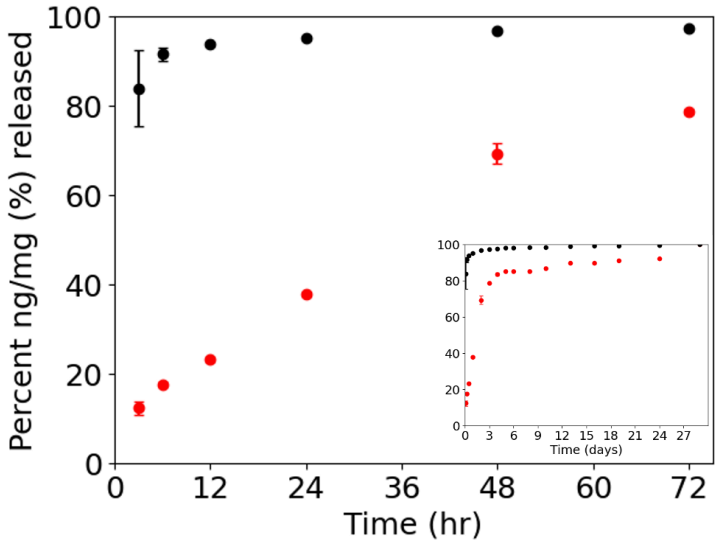

Figure 4. IgG-FITC release profile Formulation 1 (red) and Formulation 2 (black). N=3.

4. Discussion

Dynamic light scattering was attempted to measure the size distribution of the antibody-loaded particles. Due to the collapsed and non-spherical conformation of the particles, it was difficult to produce an accurate measurement of the size distribution using this method. ImageJ was used as an alternative and to measure particle circumference. Measurements of fifty particles demonstrated that Fomulation 1 averaged particles with smaller diameter compared to Fomulation 2, consistent with literature on the impact of increased flow rate on microparticle size [19]. Both Formulations 1 and 2 exhibited a similar negative zeta potential.

 doi:10.20944/preprints202405.1354.v1

The SEM images of the microparticles fabricated show a collapsed non-spherical morphology for Formulation 1 and a collapsed and discoidal morphology for Formulation 2. It is likely that the morphology observed in SEM images is a result of aqueous core solvent evaporation prior to complete PLGA shell hardening. The function of particle morphology is application-dependent. Large discoidal particles can target tumor tissue through vascular adhesion. More specifically, discoidal particles are more likely than spherical particles to localize intratumorally through margination in the tumor vasculature [23]. Further studies are needed to investigate if a discoidal particle morphology like the one produced in Formulation 2 could improve localized immune checkpoint blockade delivery in tumors.

Fluorescence images suggest localization of the antibody with the particles. In Formulation 1, it appears that the fluorescence signal is in the core. In Formulation 2, the fluoresence image suggests there is antibody localized in the shell of the particles.

It was hypothesized that coaxial electrospray of IgG-FITC at its isoelectric point with PLGA shell solution would favor IgG-FITC encapsulation in the core of PLGA microparticles. Though the results suggest this was achieved in Formulation 1, it is unclear why the encapsulation efficiency was low. It is also unclear how increased shell flow rate improved encapsulation efficiency in Formulation 2, yet without the core localization anticipated with the isoelectric point.

During Taylor cone formation, the core and shell solutions come into contact. The miscibility of water in the aqueous core with ethyl acetate in the shell influences how the two solvents interact during this time. In the solution flow rates of Formulation 1, there is a higher water:ethyl acetate volume ratio than in Formulation 2. In Formulation 1, it is possible that ethyl acetate in the shell reached water saturation because ethyl acetate is only partially water miscible. In Formulation 2, a higher flow rate of the shell solution reduce the water:ethyl acetate ratio, thereby increasing the amount of water that is able to be absorbed by the ethyl acetate solution. The absorption of water by the shell solution could explain why is antibody solute was localized in the shell region. This may also explain the increased encapsulation efficiency measured in Formulation 2. The aqueous miscibility of shell solvent may be an underapprecated consideration in the development of polymer shell / biomolecule core sustained delivery systems fabricated by coaxial electrospray.

IgG-FITC localization observed in each Formulation is consistent with the measured release profiles. Antibody encapsulated in the core was released more gradually whereas antibody apparently located near the shell demonstated greater burst-release.

Our findings suggest that in the antibody-encapsulation of IgG-FITC in PLGA microparticles using coaxial electrospray, core-shell solvent interactions may influence encapsulation, antibody localization, and release profiles, even at the antibody's isoelectric point.

Supplementary Materials: The following supporting information can be downloaded at: Preprints.org.

Author Contributions: Conceptualization, Karla Robles, Richard Mu and Todd Giorgio; Data curation, Karla Robles; Formal analysis, Karla Robles and John Libanati; Funding acquisition, Karla Robles, Richard Mu and Todd Giorgio; Investigation, Karla Robles, John Libanati, Richard Mu and Todd Giorgio; Methodology, Karla Robles, John Libanati and Richard Mu; Project administration, Karla Robles and Todd Giorgio; Resources, Richard Mu and Todd Giorgio; Supervision, Richard Mu and Todd Giorgio; Visualization, Karla Robles and John Libanati; Writing – original draft, Karla Robles; Writing – review & editing, Richard Mu and Todd Giorgio.

Funding: This research was funded by the National Science Foundation Graduate Research Fellowship Program (Award number: 2240920), the DMR Partnerships for Research and Education in Materials Research (PREM) (Awrd number: DMR-2122169), and the National Institutes of Health (Project number: U54MD007586-37).

Institutional Review Board Statement: Not applicable.

Data Availability Statement: The raw data supporting the conclusions of this article will be made available by the authors on request.

Acknowledgments: In this section, you can acknowledge any support given which is not covered by the author contribution or funding sections. This may include administrative and technical support, or donations in kind (e.g., materials used for experiments).

Conflicts of Interest: The authors declare no conflicts of interest.

 doi:10.20944/preprints202405.1354.v1

References

1. Jin, Q.; Liu, Z.; Chen, Q; Controlled release of immunotherapeutics for enhanced cancer immunotherapy after local delivery. *J. Controlled Release.* **2021**, *329*, 882–893.
2. Chen Q.; Chen G.; Chen J.; et al. Bioresponsive Protein Complex of aPD1 and aCD47 Antibodies for Enhanced Immunotherapy. *Nano Lett.* **2019**, *19*(8).
3. Wang C.; Sun W.; Wright G.; et al; Inflammation-Triggered Cancer Immunotherapy by Programmed Delivery of CpG and Anti-PD1 Antibody. *J. Adv Mater*. **2016**, *28*(40).
4. Awwad S.; Angkawinitwong U.; Overview of Antibody Drug Delivery. *Pharmaceutics*. **2018**, *10*(3). .
5. Riley R.S.; June C.H.; Langer R.; Mitchell M.J.; Delivery technologies for cancer immunotherapy. *Nat. Rev. Drug Discov*. **2019**, *18*(3).
6. Danckwerts M.; Fassihi A.; Implantable controlled release drug delivery systems: A review. *Drug Dev. Ind. Pharm*. **1991**, *17*(11).
7. Geraili A.; Xing M.; Mequanint K.; Design and fabrication of drug-delivery systems toward adjustable release profiles for personalized treatment. *View*. **2021**; *2*(5). https://doi.org/10.1002/VIW.20200126.
8. Makadia H.K.; Siegel S.J.; Poly Lactic-co-Glycolic Acid (PLGA) as biodegradable controlled drug delivery carrier. *Polym*ers. **2011**, 3(3). https://doi.org/10.3390/polym3031377.
9. Kapoor D.N.; Bhatia A.; Kaur R.; Sharma R.; Kaur G.; Dhawan S.; PLGA: A unique polymer for drug delivery. *Ther. Deliv.* **2015**, 6(1). https://doi.org/10.4155/tde.14.91.
10. Su Y.; Zhang B.; Sun R.; et al; PLGA-based biodegradable microspheres in drug delivery: Recent advances in research and application. *Drug Deliv*. **2021**, 28(1). https://doi.org/10.1080/10717544.2021.1938756.
11. Yoo J.; Won Y.Y.; Phenomenology of the Initial Burst Release of Drugs from PLGA Microparticles. *ACS Biomater. Sci. Eng*. **2020**, 6(11). https://doi.org/10.1021/acsbiomaterials.0c01228.
12. Alfatama M.; Shahzad Y.; Choukaife H.; Recent advances of electrospray technique for multiparticulate preparation: Drug delivery applications. *Adv. Colloid. Interfac*. **2024**, 325. https://doi.org/10.1016/J.CIS.2024.103098.
13. Ramazani F.; Chen W.; van Nostrum C.F.; et al; Strategies for encapsulation of small hydrophilic and amphiphilic drugs in PLGA microspheres: State-of-the-art and challenges. *Int. J. Pharm*. **2016**, *499(1-2),* 358-367. https://doi.org/10.1016/J.IJPHARM.2016.01.020.
14. Zhai P.; Chen X.B.; Schreyer D.J.; PLGA/alginate composite microspheres for hydrophilic protein delivery. *Mater. Sci. Eng. C*. **2015**, *56*, 251–259. https://doi.org/10.1016/j.msec.2015.06.015.
15. Yasmin F.; Chen X.; Eames B.F.; Effect of process parameters on the initial burst release of protein-loaded alginate nanospheres. *J. Func. Biomater*. **2019**, *10(3). https://doi.org/*10.3390/jfb10030042.
16. Moreira A.; Lawson D.; Onyekuru L.; Dziemidowicz K.; Angkawinitwong U.; Costa P. F.; Radacsi, N.; & Williams G. R.; Protein encapsulation by electrospinning and electrospraying. *J. Control. Release* **2021**, *329.* https://doi.org/10.1016/j.jconrel.2020.10.046.
17. Nie H.; Dong Z.; Arifin D.Y.; Hu Y.; & Wang C.H; Core/shell microspheres via coaxial electrohydrodynamic atomization for sequential and parallel release of drugs. *J. Biomed. Mater. Res. A*, **2010**, *95*(3A). https://doi.org/10.1002/jbm.a.32867.
18. Valo H.; Peltonen L.; Vehviläinen S.; Karjalainen, M.; Kostiainen R.; Laaksonen T.; & Hirvonen, J. Electrospray encapsulation of hydrophilic and hydrophobic drugs in poly(L-lactic acid) nanoparticles. *Small*, **2009**, *5*(15). https://doi.org/10.1002/smll.200801907.
19. Morais A.S.; Vieira E.G.; Afewerki S.; et al. Fabrication of polymeric microparticles by electrospray: The impact of experimental parameters. *J. Func. Biomater.* **2020**, *11(1). https://doi.org/*10.3390/jfb11010004.
20. Yuan S.; Lei F.; Liu Z.; Tong Q.; Si T.; Xu R.X.; Coaxial electrospray of curcumin-loaded microparticles for sustained drug release. *PLoS ONE.* **2015**, *10(7). https://doi.org/*10.1371/journal.pone.0132609.
21. Tang C.; Ozcam A.E.; Stout B.; Khan S.A.; Effect of pH on protein distribution in electrospun PVA/BSA composite nanofibers. *Biomacromolecules*. **2012**, *13(5). https://doi.org/*10.1021/bm2017146.
22. Angkawinitwong U.; Awwad S.; Khaw P.T.; Brocchini S.; Williams G.R.; Electrospun formulations of bevacizumab for sustained release in the eye. *Acta Biomater*. **2017**, *64. https://doi.org/*10.1016/j.actbio.2017.10.015.
23. Wang Z.; Wu Z.; Liu J.; Zhang W.; Particle morphology: An important factor affecting drug delivery by nanocarriers into solid tumors. *Expert Opin. Drug Deliv*. **2018**, *15(4). https://doi.org/*10.1080/17425247.2018.1420051.